

An orbital-selective spin liquid in a frustrated heavy fermion spinel LiV_2O_4

Yasuhiro Shimizu*,¹ Hikaru Takeda,¹ Moe Tanaka,¹ Masayuki Itoh,¹ Seiji Niitaka,² and Hidenori Takagi²

¹Department of Physics, Graduate School of Science, Nagoya University, Furo-cho, Chikusa-ku, Nagoya 464-8602, Japan

²RIKEN Advanced Science Institute, 2-1, Hirosawa, Wako, Saitama 351-0198, Japan

(Dated: February 23, 2018)

The pronounced enhancement of the effective mass is the primary phenomenon associated with strongly correlated electrons. In the presence of local moments, the large effective mass is thought to arise from Kondo coupling, the interaction between itinerant and localised electrons. However, in d electron systems, the origin is not clear because of the competing Hund's rule coupling. Here we experimentally address the microscopic origin for the heaviest d fermion in a vanadium spinel LiV_2O_4 having geometrical frustration. Utilising orbital-selective ^{51}V NMR, we elucidate the orbital-dependent local moment that exhibits no long-range magnetic order despite persistent antiferromagnetic correlations. A frustrated spin liquid, Hund-coupled to itinerant electrons, has a crucial role in forming heavy fermions with large residual entropy. Our method is important for the microscopic observation of the orbital-selective localisation in a wide range of materials including iron pnictides, cobaltates, manganites, and ruthnates.

PACS numbers:

Introduction

Electrons in metals behave as quasiparticle dressing interactions. The mass of quasiparticles often becomes extremely heavy when metallic phases are close to the quantum critical boundary for the insulating or magnetic phase¹. The microscopic understanding of heavy quasiparticles (HQs) has been a goal of modern many-body quantum statistics. An established route for HQs is antiferromagnetic Kondo coupling between localised f spins and itinerant electrons in rare-earth metals. In contrast to the f -electron case, the presence of localised spins is not apparent for d -electron systems. Alternative routes driving d HQ formation have been challenging issues in strongly correlated electron physics.

A representative d HQ material is the vanadium spinel LiV_2O_4 (Ref. 2,3), which has a highly-frustrated pyrochlore lattice for the B site $\text{V}^{3.5+}$ ($3d^{1.5}$) ions (Fig. 1a). Anisotropic orbital-dependent intersite interactions give an itinerant e'_g orbital and a more localised a_{1g} orbital through a small trigonal distortion of the VO_6 octahedron (Fig. 1b)^{4,5}. The HQ was initially explained by off-site Kondo exchange interactions, J_K , between localised a_{1g} moments and itinerant e'_g electrons (Fig. 1b)⁴. In the t_{2g} manifold, however, the strong on-site ferromagnetic Hund's exchange interaction, J_H , can overcome J_K . Many alternative scenarios such as geometrical frustration via antiferromagnetic interactions J_{AF} ,⁶⁻⁸ electron correlations^{9,10}, and spin-orbital fluctuations^{11,12} have been proposed.

Experimentally, the interpretations have been unclear for HQs in LiV_2O_4 . Charge-sensitive probes such as resistivity², photoemission¹³, and optical¹⁴ measurements showed crossover from a high-temperature incoherent metal to a low-temperature Fermi liquid across the characteristic temperature $T^* \sim 20\text{-}30$ K. In contrast, spin-sensitive probes including static spin susceptibility^{2,15} and inelastic neutron scattering¹⁶ measurements imply local moments with antiferromagnetic correlations at low temperatures. Furthermore anomalous temperature T dependences on the specific heat

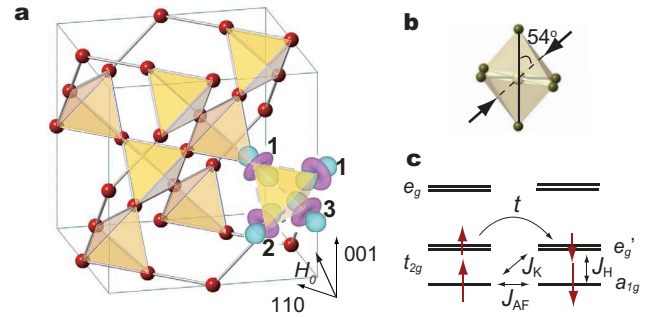


FIG. 1: **V pyrochlore lattice and exchange interactions between $3d$ orbitals in LiV_2O_4 .** (a) Corner-sharing V-tetrahedra offer geometric frustration against magnetic ordering. In the cubic lattice with local trigonal distortion, three vanadium sites with a_{1g} -like orbitals, numbered 1, 2, and 3 are not equivalent to the magnetic field H_0 rotated from the [001] to [110] axis. (b) A trigonally distorted VO_6 ligand field splits a five-fold $3d$ level into e_g and t_{2g} having lower a_{1g} and upper e'_g with 1.5 electrons. For the 2 and 3 sites, the trigonal axis is located at 54° measured from the crystal [001] axis. (c) In a Kondo lattice having localised a_{1g} and itinerant e'_g electrons with transfers t , exchange interactions between the occupied orbitals are composed of the on-site ferromagnetic Hund's coupling J_H , the off-diagonal Kondo coupling J_K , and the off-site antiferromagnetic kinetic exchange J_{AF} .

C/T and the Hall coefficient conflict with those expected in a conventional Fermi liquid². Despite the theoretical view of orbital-selective interactions, no experimental effort has been made to detect the orbital degrees of freedom.

Here, we address the first experimental approach for microscopic observations of the d HQ via orbital-resolved nuclear magnetic resonance (ORNMR) measurements in LiV_2O_4 . The previous NMR experiments using closed-shell Li sites^{2,15} only measured the net spin susceptibility proportional to the bulk value because the hyperfine interactions at the Li site surrounded by 12 vanadium sites average out the anisotropy. Our ORNMR spectroscopic approach using on-site ^{51}V spins on a high-quality single crystal is sensitive to the orbital-

dependent local spin susceptibility, which is beneficial for probing strongly correlated electrons with the orbital degrees of freedom.

Results

ORNMR Knight shift. In LiV_2O_4 the spin susceptibility χ^s consists of the a_{1g} and e'_g components: $\chi^s = \chi^a + \chi^e$ (hereafter the superscripts a and e denote a_{1g} and e'_g , respectively). The NMR frequency shift called the Knight shift, $\mathbf{K}^s = (K_x^s, K_y^s, K_z^s)$ (x , y , and z are the principal axes), measures the spin susceptibility via the hyperfine interaction $\mathcal{H}_n = \sum_i \mathbf{I} \cdot \mathbf{A}_i \cdot \tilde{\mathbf{s}}_i$ with the hyperfine coupling tensor \mathbf{A}_i between the nuclear spin \mathbf{I} and the paramagnetic spin polarisation $\tilde{\mathbf{s}}_i$ for the i -th electron under an external magnetic field. Whereas the isotropic shift $K_{\text{iso}}^s = (K_z^s + 2K_x^s)/3$ due to the core polarization is proportional to χ^s , the anisotropic part $K_{\text{ax}}^s = 2(K_z^s - K_x^s)/3$ due to the orbital-specific dipole hyperfine interaction¹⁷ is expressed by using the principal z component of the coupling constants, A_z^a and A_z^e ,

$$K_{\text{ax}}^s = \frac{1}{N\mu_B} (A_z^a \chi^a + A_z^e \chi^e), \quad (1)$$

where N is Avogadro's number and μ_B is the Bohr magneton. In contrast to K_{iso}^s , K_{ax}^s measures the hyperfine-weighted average of the orbital-dependent spin susceptibility. In the ionic limit, A_z^a and A_z^e are given by a quadratic combination of the angular momentum (see Methods) with the reversed sign and the same amplitude, $A_z^a = -A_z^e > 0$ (Ref. 17). Hence, we can distinguish which orbital dominates the spin susceptibility from the sign of K_{ax}^s and obtain the orbital occupation from the amplitude. Namely, K_{ax}^s should be positive (negative) for $\chi^a > \chi^e$ ($\chi^a < \chi^e$).

The ^{51}V Knight shift tensors of LiV_2O_4 are determined from the angle dependence of K for 2-300 K, as shown in Fig. 2. The ^{51}V NMR spectra were detectable only at specific angles, where the nuclear quadrupole interaction almost vanishes, because the nuclear spin-spin relaxation times at other angles are too fast. The obtained K traces three cosine curves of Eq. (2) in the Methods, which satisfies the cubic $Fd3m$ lattice. The principal z axis of K at $\pm 54^\circ$ for the two V sites indicates the $3d$ orbital symmetry governed by the trigonal VO_6 crystal field (Fig. 1b). At 300 and 2 K the relationship $K_z^s > K_x^s$ ($K_{\text{ax}}^s > 0$) shows the a_{1g} -dominant spin susceptibility ($\chi^a > \chi^e$). The result is consistent with the localised nature of the a_{1g} orbital, as theoretically suggested^{4-6,10}.

Temperature dependence of orbital occupations. To address HQ formation, we measured the thermal variations of the ^{51}V Knight shifts K_{iso}^s and $-K_{\text{ax}}^s$ in comparison with the ^7Li Knight shift $^7K^s$ and the bulk spin susceptibility χ (Fig. 3a). Good linearity was observed between these Knight shifts and χ (Fig. S1). All of data show a Curie-Weiss-like increase at high temperatures, followed by a broad maximum at approximately 20 K. The results agree with the spin susceptibility for high-quality crystals, free from a Curie-tail increase at low temperatures^{2,3}. The on-site ^{51}V Knight shift probes

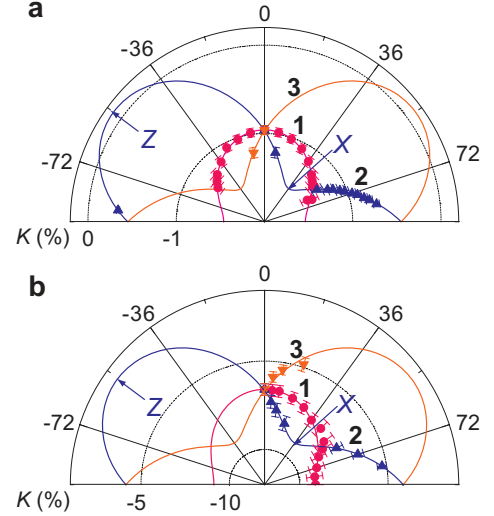


FIG. 2: **Angle dependence of the ^{51}V Knight shift K of LiV_2O_4 at (a) 300 K and (b) 2 K.** K is plotted against the magnetic field direction measured from the $[001]$ axis to the orthogonal $[110]$ axis. The K data with different colors and symbols arise from three vanadium sites **1**, **2**, and **3** due to different orbital configurations against the external magnetic field and trace three curves of the general formula, as shown in Eq. (2). Error bar is defined by a standard deviation of the Lorentzian fit of the NMR spectra. The principal Z and X axes of K for **2** and **3** are respectively located at $\mp 54^\circ$ and $\pm 36^\circ$ measured from $[001]$.

the spin susceptibility with greater sensitivity than the off-site ^7Li one and shows a smooth decrease below T^* . Below 5 K K^s becomes nearly T -independent, as observed in the Fermi liquid.

When a_{1g} local moments becomes Fermi liquid with HQ via a_{1g} - e'_g hybridisation or intersite Kondo coupling below T^* , χ^a is expect to decrease significantly, whereas χ^e is less sensitive. It could lead a decrease of K_{ax}^s from Eq. (1). To inspect this property, we plot $K_{\text{ax}}^s/K_{\text{iso}}^s \equiv \tilde{q}_{zz}$ against T in Fig. 3b. We find no appreciable change in \tilde{q}_{zz} for 2-300K. This lack of change signifies that the localised character of the a_{1g} orbital persists to the Fermi liquid state across T^* . Although \tilde{q}_{zz} of the f -electron system has not been reported, the nonlinear relationship in the K - χ plot may be a manifestation of Kondo coupling in the Ce and U-based compounds²⁰⁻²².

\tilde{q}_{zz} reflects the $3d$ orbital polarisation when χ^a and χ^e scale to electron occupations. From $\tilde{q}_{zz} = -0.7$ we can evaluate the mixing ratio of the a_{1g} and e'_g orbitals in LiV_2O_4 . The singly occupied a_{1g} orbital has $\tilde{q}_{zz} = -1.2$, as observed in the insulating pyrochlore material $\text{Lu}_2\text{V}_2\text{O}_7$ (Ref. 18). In contrast, \tilde{q}_{zz} vanishes for equivalent mixing of a_{1g} and e'_g , as observed in a less correlated metal V_2O_3 (Fig. 3b). The observed intermediate \tilde{q}_{zz} in LiV_2O_4 manifests a significant e'_g contribution to the spin susceptibility in throughout the temperature range. Namely, the e'_g spin must be polarised via Hund's rule coupling to the localised a_{1g} spins under the magnetic field, although the itinerancy of e'_g is much better than that of a_{1g} . The occupation ratio is evaluated as $a_{1g} : e'_g = 4 : 1$ (see Methods), corresponding to the electron numbers of $n_{a_{1g}} \sim 1$ and

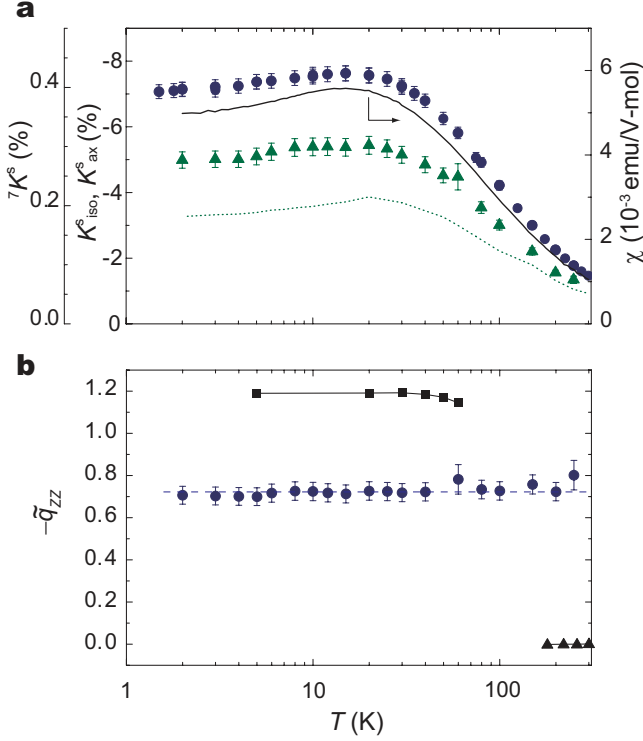


FIG. 3: **Temperature dependence of spin and orbital polarisations in LiV_2O_4 .** (a) Local spin susceptibilities probed by ${}^{51}\text{V}$ isotropic shift K_{iso}^s (circles with error bars), axially anisotropic shift $-K_{\text{ax}}^s$ (triangles with error bars), and ${}^7\text{Li}$ Knight shift ${}^7K^s$ (green dotted line), where error bars are defined by the standard deviation. The right-hand axis shows the bulk susceptibility χ (solid curve). A constant $K_0 = 0.4\%$ obtained from the K - χ plot (Fig. S1) is subtracted from K . (b) The effective $3d$ orbital polarisation \tilde{q}_{zz} (blue circle with error bars) in comparison with the fully a_{1g} polarised value $\tilde{q}_{zz,0} = -1.2$ in $\text{Lu}_2\text{V}_2\text{O}_7$ (black square)¹⁸, and the fully unpolarised value $\tilde{q}_{zz,0} = 0$ in a weakly correlated metal V_2O_3 (black circle) (Y.S., M.I., & Y. Ueda, unpublished results). \tilde{q}_{zz} is obtained from K_{ax}^s divided by K_{iso}^s to cancel the spin polarisation.

$n_{e_g} \sim 0.25$ for $3d^{1.5}$. The half-filling a_{1g} occupation is distinct from that expected in the tight-binding calculation without electron correlations, where $n_{a_{1g}} : n_{e_g} = 1 : 4$ (Ref. 12). However, it is compatible with the strongly localised a_{1g} picture due to the strong renormalization into the Mott insulating state^{5,9,10} and provides microscopic evidence for orbital-dependent localisation, which is robust across T^* .

Dynamical spin susceptibility of the orbital-selective spin liquid Another interesting issue is the dynamical part probed by the nuclear spin-lattice relaxation rate T_1^{-1} . $(T_1T)^{-1}$ is generally given by $(T_1T)^{-1} \sim \sum_{\mathbf{q}} |A_{\perp}(\mathbf{q})|^2 \text{Im}\chi_{\perp}(\mathbf{q}, \omega)/\omega$ (Ref. 19), where $A_{\perp}(\mathbf{q})$ is the wave vector \mathbf{q} component of the hyperfine coupling constant normal to the quantization axis, and $\chi_{\perp}(\mathbf{q}, \omega)$ is the transverse dynamical spin susceptibility at the NMR frequency ω . In a cubic lattice, $A_{\perp}(\mathbf{q})$ and $\chi_{\perp}(\mathbf{q}, \omega)$ are isotropic for the ${}^{51}\text{V}$ and ${}^7\text{Li}$ sites. $(T_1T)^{-1}$ measured for ${}^{51}\text{V}$ and ${}^7\text{Li}$ (Fig. 4a) follows the linear relationship $({}^{51}T_1T)^{-1} = C({}^7T_1T)^{-1} + C_0$, where

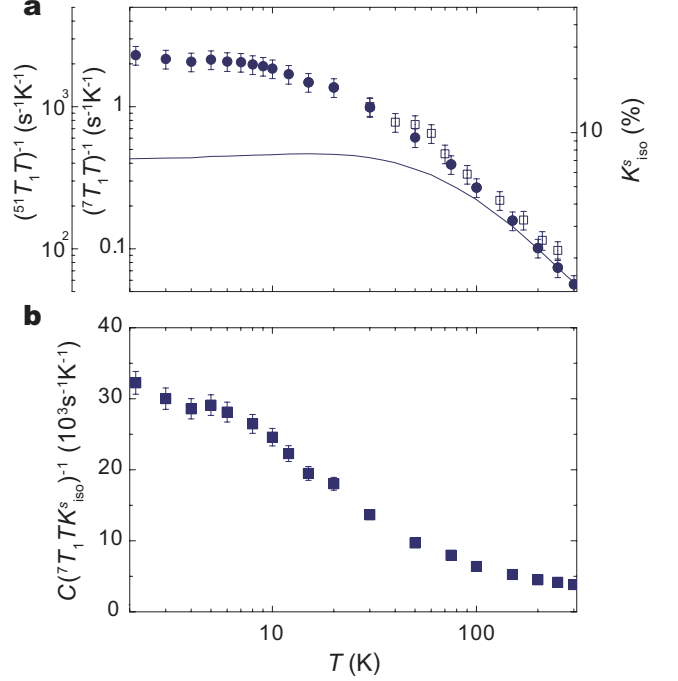


FIG. 4: **The dynamical spin susceptibility compared to a static one in LiV_2O_4 .** a, The temperature dependence of the nuclear spin-lattice relaxation rate divided by temperature T , $(T_1T)^{-1}$, obtained for ${}^7\text{Li}$ (solid circle with error bars) and ${}^{51}\text{V}$ (open square with error bars) NMR (left axes), and the isotropic ${}^{51}\text{V}$ Knight shift K_{iso}^s (solid line, right axis) in LiV_2O_4 , where error bars are defined by the standard deviation. b, $C({}^7T_1T)^{-1}$ (solid square with error bars) divided by K_{iso}^s , where $C({}^7T_1T)^{-1}$ is equivalent to the spin part of $({}^{51}T_1T)^{-1}$.

the linear coefficient $C = 1.0 \times 10^3$ is close to the square ratio of the hyperfine coupling, $\frac{({}^{51}\gamma^s A_{\text{iso}}^s)^2}{({}^7\gamma^s A_{\text{iso}}^s)^2} = 1.1 \times 10^3$ and $C_0 = 64 \text{ s}^{-1}\text{K}$ arises from the T -invariant orbital component. The scaling relation indicates that the Li sites probe spin fluctuations via the transferred hyperfine interaction and allows us to evaluate unobservable $({}^{51}T_1T)^{-1}$ at low temperatures from $({}^7T_1T)^{-1}$.

In the present case, $(T_1T)^{-1}$ is governed by paramagnetic fluctuations of local moments at high temperatures. Above 150 K the scaling behaviour between $({}^7T_1T)^{-1}$ and K_{iso}^s is indeed observed ($C({}^7T_1TK_{\text{iso}}^s)^{-1} = \text{constant}$ in Fig. 4b). Below 150 K a progressive $({}^7T_1T)^{-1}$ increase indicates antiferromagnetic correlation, consistent with the growth of $\chi(\mathbf{q}, \omega)$ at a finite \mathbf{q} ($= 0.64^{-1}$) in the inelastic neutron scattering measurements below 80 K (Ref. 16). Therefore the suppression of χ^s at low temperatures likely comes from the short-range antiferromagnetic correlation with the exchange interaction $J_{\text{AF}} \sim 150$ K. Nevertheless, no long-range magnetic ordering occurs down to 1.5 K, the energy scale of $\sim J_{\text{AF}}/100$. It suggests that the frustrated a_{1g} spins form in a quantum liquid at low temperatures with low-lying excitations.

Discussion

Our results provide significant insights into the formation of $3d$ HQ. As observed in the T -independent \tilde{q}_{zz} , the a_{1g} spins likely remain incoherent, even entering into a coherent 'Fermi liquid' state, and couple ferromagnetically to e'_g spins. No indication of Kondo coupling was observed down to low temperatures despite the large antiferromagnetic fluctuations. The remaining local moments can be highly frustrated and carry large residual entropy⁶⁻⁸. The itinerant e'_g electrons interact with the underlying spin liquid via the Hund's rule coupling. Thus the $3d$ HQ behaviour in LiV_2O_4 could be mapped on the frustrated ferromagnetic Kondo lattice.

In the absence of antiferromagnetic Kondo coupling, the HQ formation has not established theoretically. In a Hubbard model calculation, the Kondo-like coherence peak appears on the boundary of the orbital-selective Mott transition for the a_{1g} part¹⁰. Even in such a case, χ^a may vary across T^* , while χ^e be invariant. Our results suggest that, if the Kondo-like peak appears, a large fraction of the incoherent spins still remains and carries entropy. Such fractionalisation of the nearly localised electron might be common to strongly correlated electron systems²³ where localised and itinerant characters coexist. Furthermore, the chirality degrees of freedom might provide appreciable entropy in the pyrochlore lattice²⁴ and contribute to the anomalous Hall effect³.

The ORNMR technique offers new holographic experiments that could give microscopic insights into strongly correlated electrons. Various orbital-resolved tools, such as X-ray absorption and photoemission spectroscopy, have been recently developed. The Knight shift measurement has a unique advantage in detecting the orbital-dependent local spin susceptibility via the magnetic hyperfine interactions between d spins and on-site nuclear spins. The method has not been achieved in rare-earth heavy fermion compounds because of the difficulty in detecting NMR signals for the on-site nuclear spins²⁰. Additional technical improvements in the NMR mea-

surements may reveal the hidden orbital-selective Mott transition in transition metal oxides, such as ruthenates, pnictides, and manganites.

Methods

NMR measurements. The ORNMR experiments were performed on a single crystal of LiV_2O_4 synthesised by the self-flux method²⁵. The crystal with the octahedral shape was placed on a two-axis goniometer and rotated under a fixed magnetic field $H_0 = 9.402$ and 8.490 T. The NMR spectra were obtained from spin-echo signals after two $\pi/2$ pulses separated by a time τ . The ^{51}V NMR measurements were made only for powder samples above 50 K (Ref. 15) likely due to the fast spin-echo decay time T_2 at low temperatures. To overcome this problem, we used a short $\tau = 3 - 10 \mu\text{s}$ and a magnetic field precisely ($<0.1^\circ$) aligned to the crystal axis equivalent to the magic angle of the nuclear quadrupole interaction. Otherwise, the NMR signals were depressed owing to the fast T_2 .

The angular dependence of the ^{51}V Knight shift $K(\theta)$ with the local trigonal symmetry is fitted into the general formula²⁶

$$K = K_{\text{iso}} - \frac{(K_z - K_x)}{6} \sin 2\theta \quad (2)$$

for the V1 site and

$$K = K_{\text{iso}} \pm \frac{(K_z - K_x)}{2} \cos(2\theta \pm 54.7^\circ) \quad (3)$$

for the V2 or V3 site related by a mirror symmetry, where $K_{\text{iso}} = \frac{K_z + 2K_x}{3}$.

Magnetic hyperfine interactions. Magnetic hyperfine interactions between $3d$ electron spins and nuclear spins, and the analysis of the ^{51}V Knight shift in LiV_2O_4 . Magnetic hyperfine interactions in $3d$ systems are generally given by¹⁷

$$\mathcal{H}_n = \mathcal{P} \sum_i \left[\mathbf{l}_i \cdot \mathbf{I} - \kappa \mathbf{s}_i \cdot \mathbf{I} - \frac{2}{(2l_i - 1)(2l_i + 3)} \left\{ \frac{3}{2} (\mathbf{l}_i \cdot \mathbf{s}_i) (\mathbf{l}_i \cdot \mathbf{I}) + \frac{3}{2} (\mathbf{l}_i \cdot \mathbf{I}) (\mathbf{l}_i \cdot \mathbf{s}_i) - l_\alpha (l_i + 1) (\mathbf{I} \cdot \mathbf{s}_i) \right\} \right] \quad (4)$$

where \mathbf{l}_i , \mathbf{s}_i , and \mathbf{I} denote operators of orbital and spin of the i -th electron, and the nuclear spin, respectively, the coefficient $\mathcal{P} = 2\mu_B \gamma_n \hbar \langle r^{-3} \rangle$ using the Bohr magneton μ_B , the nuclear gyromagnetic ratio γ_n , the Plank's constant \hbar , and a radial expectation value $\langle r^{-3} \rangle$. The first term represents the orbital contribution that quenches in crystals but partly revives via the Van-Vleck process under the magnetic field. The second term arises from a Fermi contact interaction due to the core polarisation of inner s spins, giving the isotropic hyperfine coupling constant $A_{\text{iso}}^s = -\mathcal{P} \kappa \delta_{ij}$, where κ is a dimensionless parameter ($\kappa \sim 0.5$ for vanadates¹⁸). The third term denotes anisotropic dipole interactions determined by $3d$ orbital

occupations, where the principal components are expressed as $A_{\alpha\beta}^{\text{dip}} = 2\mathcal{P}(-q_{\alpha\beta} + \lambda \Lambda'_{\alpha\beta})/7$ by using the equivalent operator of $3d$ angular momentum,

$$q_{\alpha\beta} = \frac{1}{2}(l_\alpha l_\beta + l_\beta l_\alpha) - \frac{1}{3}l(l+1)\delta_{\alpha\beta}, \quad (5)$$

with the spin-orbit coupling parameter λ , and the second-order matrix elements between the ground and excited states, $\Lambda'_{\alpha\beta}$. In the LS -coupling the sum of the terms for several electrons can be replaced by

$$\mathcal{H}_n = \mathcal{P} \mathbf{L} \cdot \mathbf{I} - \mathcal{P} \kappa \mathbf{S} \cdot \mathbf{I} - \mathcal{P} \left[\frac{3}{2} \xi \{ (\mathbf{L} \cdot \mathbf{S})(\mathbf{L} \cdot \mathbf{I}) + (\mathbf{L} \cdot \mathbf{I})(\mathbf{L} \cdot \mathbf{S}) \} - \xi L(L+1)(\mathbf{I} \cdot \mathbf{S}) \right], \quad (6)$$

where \mathbf{L} and \mathbf{S} are total orbital and spin, respectively, and

$$\xi = \frac{2l+1-4s}{5(2l-1)(2l+3)(2l-1)} = \frac{2}{21} \text{ for } 3d^1.$$

The experimental observable is the Knight shift tensor $\mathbf{K} = (K_x, K_y, K_z)$ defined as the resonance frequency shift due to the hyperfine interaction of Eq. (4). The spin component K^s is obtained by subtracting the small orbital component K_0 including the chemical shift and the Van-Vleck shift from the K - χ plot in Fig. S1. For a paramagnetic system, \mathbf{s}_i in Eq. (4) is replaced by the effective electron spin polarization \tilde{s}_i proportional to spin susceptibility χ^s . In a multi-orbital system, χ^s is composed of orbital-dependent spin susceptibilities. Then K^s is expressed by the sum of hyperfine fields from $3d$ spins. Whereas the isotropic part of K^s , $K_{\text{iso}}^s \equiv (2K_x^s + K_z^s)/3$, is given by

$$K_{\text{iso}}^s = -\frac{\kappa}{N\mu_B} \mathcal{P} \chi^s, \quad (7)$$

the anisotropic part, $K_{\text{ax}}^s \equiv 2(K_z^s - K_x^s)/3$, is expressed as the arithmetic average of the orbital-dependent spin susceptibility weighted by the principal z component of the hyperfine coupling tensor, as shown in Eq. (1). In LiV_2O_4 with a local trigonal distortion, 1.5 electrons are filled in two orbitals, a_{1g} and e'_g , whose $q_{\alpha\beta}$ are equivalent to those of $d_{3z^2-r^2}$ and $d_{x^2-y^2}$, respectively, taking the principal axes along the trigonal axis: $q_{xx} = q_{yy} = 1$, $q_{zz} = -2$ for $(a_{1g})^1$, while the values are numerically the same but reversed in sign for $(e'_g)^2$. $q_{\alpha\alpha}$ vanishes when the two orbitals are equally occupied. Using the relation $A_z^a = -A_z^e (= -\frac{4}{7}\mathcal{P})$, K_{ax}^s is expressed as

$$K_{\text{ax}}^s \simeq \frac{1}{N\mu_B} A_z^a (\chi^a - \chi^e). \quad (8)$$

The good linearity in K - χ plots indicates $\chi^s = \chi^a + \chi^e \sim f\chi^s + (1-f)\chi^s$, where f is the fraction of χ^a in χ^s . Then K_{ax}^s can be further reduced to

$$K_{\text{ax}}^s = -\frac{4}{7N\mu_B} \mathcal{P} \chi^s (2f - 1). \quad (9)$$

for the negligible $\lambda\Lambda'_{ij}$, as expected from the small K_0 . To experimentally obtain the effective orbital polarization \tilde{q}_{zz} , we take a ratio of Eqs. (7) and (9) and cancel out the numerical constants and χ^s . Namely,

$$\frac{K_{\text{ax}}^s}{K_{\text{iso}}^s} \simeq -\frac{8}{7}(2f - 1) \equiv \tilde{q}_{zz}. \quad (10)$$

Here $\tilde{q}_{zz} = -8/7$ for a fully a_{1g} polarized case ($f = 1$), close to the experimentally obtained $\tilde{q}_{zz} \simeq -1.2$ in LuV_2O_7 (Ref. 18). From the experimental result $\tilde{q}_{zz} \sim -0.7$ in LiV_2O_4 , we obtained $f \sim 0.8$, corresponding to the occupation ratio $a_{1g} : e'_g = 4 : 1$ and hence $n \sim 1$ for a_{1g} and $n \sim 0.25$ for e'_g .

Electric hyperfine interactions The electrostatic hyperfine interaction can be a direct probe for $3d$ orbital order. In the presence of the anisotropic electric field gradient around the nuclear spin, the ^{51}V NMR spectrum is split into seven lines for $I = 7/2$. The NMR spectrum becomes sharpest at $[001]$, identifying the magic angle where the nuclear quadrupole splitting frequency $\delta\nu$ vanishes. Then $\delta\nu$ should have a maximum at $\theta_0 = 54.7^\circ$ satisfying $\delta\nu \sim (3\cos^2\theta_0 - 1) = 0$, which exactly equivalent to the local trigonal symmetry. We observed a quadrupole splitting frequency $\delta\nu_x = 90$ kHz in the ^{51}V NMR spectra at $H_0 \parallel [110]$, by using a very short pulse interval time $\tau = 3 \mu\text{s}$. From the lattice symmetry, we can obtain $\nu_Q \equiv 2\delta\nu_x = 180$ kHz. We confirmed that $\delta\nu_x$ was independent of temperature down to 2 K and hence the orbital occupation was invariant across T^* .

References

- ¹ Gegenwart, P. Si, Q. & Steglich, F. Quantum criticality in heavy-fermion metals. *Nat. Phys.* **4**, 186-197 (2008).
- ² Kondo, S. *et al.* LiV_2O_4 : a heavy fermion transition metal oxide. *Phys. Rev. Lett.* **78**, 3729-3733 (1997).
- ³ Urano, C. *et al.* LiV_2O_4 spinel as a heavy-mass Fermi liquid: anomalous transport and role of geometrical frustration. *Phys. Rev. Lett.* **85**, 1052-1055 (2000).
- ⁴ Anisimov, A. I. *et al.* Electronic structure of the heavy fermion metal LiV_2O_4 . *Phys. Rev. Lett.* **83**, 364-367 (1999).
- ⁵ Nekrasov, I. A. *et al.* Orbital state and magnetic properties of LiV_2O_4 . *Phys. Rev. B* **67**, 085111 (2003).
- ⁶ Lacroix, C. Heavy fermion behavior of itinerant frustrated systems: β -Mn, $\text{Y}(\text{Sc})\text{Mn}_2$ and LiV_2O_4 . *Can. J. Phys.* **79**, 1469-1473 (2001).
- ⁷ Burdin, S. Grepel, D. R. & Georges, A. Heavy-fermion and spin-liquid behaviour in a Kondo lattice with magnetic frustration. *Phys. Rev. B* **66**, 045111 (2002).
- ⁸ Hopkinson, J. & Coleman, P. LiV_2O_4 : frustration induced heavy fermion metal. *Phys. Rev. Lett.* **89**, 267201 (2002).
- ⁹ Kusunose, H. Yotsuhashi, S. & Miyake, K. Formation of a heavy quasiparticle state in the two-band Hubbard model. *Phys. Rev. B* **62**, 4403 (2002).
- ¹⁰ Arita, R. Held, K. Lukoyanov, A. V. & Anisimov, V. I. Doped Mott insulator as the origin of heavy fermion behaviour in LiV_2O_4 . *Phys. Rev. Lett.* **98**, 166402 (2007).
- ¹¹ Yamashita, Y. & Ueda, K. Spin-orbital fluctuations and a large mass enhancement in LiV_2O_4 . *Phys. Rev. B* **67**, 195107 (2003).
- ¹² Hattori, K. & Tsunetsugu, H. Effective Hamiltonian of a three-orbital Hubbard model on the pyrochlore lattice: Application to LiV_2O_4 . *Phys. Rev. B* **79**, 035115 (2009).
- ¹³ Shimoyamada, A. *et al.* Heavy-fermion-like state in a transition metal oxide LiV_2O_4 single crystal: indication of Kondo resonance in the photoemission spectrum. *Phys. Rev. Lett.* **96**, 026403 (2006).
- ¹⁴ Jönsson, P. E. *et al.* Correlation-driven heavy-fermion formation in LiV_2O_4 . *Phys. Rev. Lett.* **99**, 167402 (2007).
- ¹⁵ Mahajan, A. V. *et al.* ^7Li and ^{51}V NMR study of the heavy-fermion compound LiV_2O_4 . *Phys. Rev. B* **57**, 8890-8899 (1998).
- ¹⁶ Lee, S. H. *et al.* Spin fluctuations in a magnetically frustrated metal LiV_2O_4 . *Phys. Rev. Lett.* **86**, 5554-5557 (2001).

- ¹⁷ Abragam, A. & Bleaney, B. *Electron Paramagnetic Resonance of Transition Ions*, Oxford University Press, London (1970).
- ¹⁸ Kiyama, T. *et al.* Direct observation of the orbital state in $\text{Lu}_2\text{V}_2\text{O}_7$: A ^{51}V NMR study. *Phys. Rev. B* **73** 184422 (2006).
- ¹⁹ Moriya, T. The effect of the electron-electron on the nuclear spin-lattice relaxation rate in metals. *J. Phys. Soc. Jpn.* **18**, 516-520 (1963).
- ²⁰ Curro, N. J. Young, B.-L. Schmalian, J. & Pines, D. Scaling in the emergent behavior of heavy-electron materials. *Phys. Rev. B* **70**, 235117 (2004).
- ²¹ Sakai, H. Baek, *et al.* ^{59}Co NMR shift anomalies and spin dynamics in the normal state of superconducting CeCoIn_5 : Verification of two-dimensional antiferromagnetic spin fluctuations. *Phys. Rev. B* **82**, 020501R (2010).
- ²² Kambe, S. *et al.* One-component description of magnetic excitations in the heavy-fermion compound CeIrIn_5 . *Phys. Rev. B* **81**, 140405R (2010).
- ²³ Sachdev, S. Holographic metals and the fractionalized Fermi liquid. *Phys. Rev. Lett.* **105**, 151602 (2010).
- ²⁴ Udagawa, M & Motome, Y. Chirality-driven mass enhancement in the kagome Hubbard model *Phys. Rev. Lett.* **104**, 106409 (2010).
- ²⁵ Matsushita, Y. Ueda, H. & Ueda, Y. Flux crystal growth and thermal stabilities of LiV_2O_4 . *Nat. Mater.* **4**, 845-850 (2005).
- ²⁶ Volkoff, G. M. Petch, H. E. & Smellie, D. W. Nuclear electric quadrupole interaction in single crystals. *Can. J. Phys.* **30**, 270-289 (1952).

Acknowledgements

We thank technical assistance by S. Inoue, and valuable discussion with N. Kawakami, Y. Motome, S. Watanabe, T. Tsunetsugu, and S. Sachdev. This work was financially supported by the Grant-in-Aid for Scientific Research on the Priority Area, Novel State of Matter Induced by Frustration, (No. 22014006) from the MEXT, and the Grants-in-Aid for Scientific Research (No. 22684018 and 24340080) from the JSPS.